

Article

Not peer-reviewed version

Experimental Modal Testing of Lightweight Composite UAV Structures: Methods and Key Challenges

[Jakub Wróbel](#) , [Kamil Jendryka](#) , [Maciej Milewski](#) , [Artur Kierzkowski](#) , [Michał Stosiak](#) , [Olegas Prentkovskis](#) , [Mykola Karpenko](#) *

Posted Date: 14 February 2026

doi: 10.20944/preprints202602.1120.v1

Keywords: composite materials; experimental testing; unmanned aerial vehicle; structural dynamics; vibration; aerospace composites; winglet



Preprints.org is a free multidisciplinary platform providing preprint service that is dedicated to making early versions of research outputs permanently available and citable. Preprints posted at Preprints.org appear in Web of Science, Crossref, Google Scholar, Scilit, Europe PMC.

Copyright: This open access article is published under a [Creative Commons CC BY 4.0 license](#), which permit the free download, distribution, and reuse, provided that the author and preprint are cited in any reuse.

Disclaimer/Publisher's Note: The statements, opinions, and data contained in all publications are solely those of the individual author(s) and contributor(s) and not of MDPI and/or the editor(s). MDPI and/or the editor(s) disclaim responsibility for any injury to people or property resulting from any ideas, methods, instructions, or products referred to in the content.

Article

Experimental Modal Testing of Lightweight Composite UAV Structures: Methods and Key Challenges

Jakub Wróbel ¹, Kamil Jendryka ², Maciej Milewski ¹, Artur Kierzkowski ¹, Michał Stosiak ¹, Olegas Prentkovskis ³ and Mykola Karpenko ³

¹ Department of Technical Systems Operation and Maintenance, Faculty of Mechanical Engineering, Wrocław University of Science and Technology, 50-372 Wrocław, Poland

² Faculty of Mechanical and Power Engineering, Wrocław University of Science and Technology, 50-370 Wrocław, Poland

³ Faculty of Transport Engineering, Vilnius Gediminas Technical University, 10105, Vilnius, Lithuania

* Correspondence: mykola.karpenko@vilniustech.lt

Abstract

This study aims to conduct an experimental modal analysis of a very lightweight composite structure representative of UAV application and to evaluate the suitability of different testing approaches for reliable identification of its dynamics characteristics. The investigated structure is a winglet made of carbon fibre reinforced polymer (CFRP) with a lightweight foam core. The experimental campaign was based on impact hammer excitation combined with triaxial accelerometer measurements. Modal tests were performed under three different boundary conditions: free-free suspension using elastic cords, free-free approximation using compliant foam support, and fixed conditions reflecting the operational mounting of the winglet. The objective of the study is not only to identify natural frequencies and mode shapes, but primarily to assess the influence of support conditions, excitation quality and measurement-induced mass loading on the reliability of the extracted modal parameters. By comparing the obtained frequency response functions and modal characteristics across different test configurations, the work seeks to identify the most appropriate experimental approach for modal analysis of ultra-lightweight composite UAV structures, providing practical guidance for future vibration investigations.

Keywords: composite materials; experimental testing; unmanned aerial vehicle; structural dynamics; vibration; aerospace composites; winglet

1. Introduction

The proliferation of Unmanned Aerial Vehicles (UAVs) marks a significant transition in modern transport [1,2]. So-called drones extend their presence to military applications [3,4], large-area surveillance [5] and cargo delivery [6]. A key operational requirement for Mini and Small UAV platforms is maximizing flight endurance and operational range [7]. It requires usage of ultra-lightweight and structurally efficient materials. Consequently, advanced composites, particularly those based on carbon fiber (CFRP) have become the material of choice due to their superior strength-to-weight ratio and fatigue resistance compared to traditional metallic alloys [8]. To further optimize structural performance and increase bending stiffness while maintaining minimal mass, manufacturers frequently employ sandwich composite structures. These systems typically consist of high-stiffness CFRP face sheets separated by a lightweight, low-density foam core. These materials are widely used in components, like winglets, which are essential devices added to the wingtips. The primary function of these components is reduction of induced drag and enhancement of the effective aspect ratio, thereby contributing directly to improved fuel efficiency and extended operational range [9].

As UAV structures continue to decrease in mass and structural stiffness, their dynamic behavior becomes an increasingly critical design consideration. Lightweight composite components are inherently more susceptible to vibration-related phenomena, including aeroelastic instabilities such as flutter. Reliable identification of their modal properties is therefore a prerequisite for any credible dynamic or aeroelastic assessment, particularly in the early stages of design, where simplified analytical or low-order numerical models are commonly employed [10].

Maharudra et al. [11] investigated the vibration behavior of laminated composite panels with varying thickness and boundary conditions using a higher-order shear deformation theory. Their results showed that boundary conditions have a significant influence on natural frequencies for thin plate configurations, whereas this effect becomes negligible for thick plates. Their study was conducted through numerical simulations. Guo et al. [12] investigated the effect of boundary conditions on the vibration characteristics of sandwich plates with periodic cores using a theoretical and finite element approach. They showed that varying the stiffness of boundary constraints influences the vibration band structure and band-gap characteristics of the plate. Erklığ et al. [13] analyzed the influence of boundary conditions on the free vibration and damping characteristics of hybrid laminated composite plates composed of carbon, Kevlar and S-glass fibers. Their experimental and finite element results revealed that boundary constraints significantly affect both natural frequencies and damping behavior, with distinct differences observed between clamped, simply supported and free edge configurations. The study employed experimental modal testing based on impact hammer excitation and accelerometer response measurements. Qu et al. [14] investigated modal testing methods for honeycomb sandwich panels subjected to conditions relevant for aerospace applications, such as noise loads and elevated temperatures. Four excitation approaches were compared: impact hammer excitation, transient excitation, pulse sequence excitation, and random noise excitation. The study demonstrated that all four methods can provide effective modal measurement results. The experimental campaign was conducted on sandwich specimens of relatively large dimensions and mass, and the primary focus was placed on high-temperature testing conditions. Karpenko et al. [15] examined the modal response of extruded polystyrene foam embedded in composite panels, combining experimental micro-vibration measurements with finite element simulations. The study highlighted low-frequency resonances and confirmed close agreement between numerical and experimental results, emphasizing the importance of accurately characterizing lightweight materials for dynamic and aeroelastic assessments in small aircraft structures. During experiment a piezoelectric micro-actuator was used to excite controlled vibrations in XPS samples, while the dynamic surface response was captured using a laser scanning vibrometer. Zhang et al. [16] conducted an experimental and numerical investigation of the thermal-vibration behavior of lattice-structured air rudders subjected to combined thermal gradients and dynamic excitation. Modal characteristics under elevated temperatures were identified using non-contact scanning laser Doppler vibrometry with usage of an electromagnetic vibrator to excite the structure. Qaumi and Hashemi [17] performed combined experimental and numerical modal analyses of an experimental rocket aerostructure in order to assess and calibrate finite element models used in the design process. Excitation was provided by a hammer tap test, and the structural response was measured using laser Doppler vibrometers. Chuang and Kim [18] investigated the influence of uniaxial static loading on the dynamic behavior of unidirectional carbon-based composite (UCBC) structures. Their study demonstrated that static preload can significantly modify modal parameters. Uniaxial accelerometers were attached to the specimens, and excitation was provided using a modal impact hammer.

Despite the extensive range of materials, structural configurations, and testing approaches reported in the literature, no unified guidelines exist for experimental modal analysis of ultra-lightweight composite components used in mini and micro UAVs. Previous studies have explored various boundary conditions, excitation strategies, and measurement systems, yet the influence of support configuration on the identified dynamic characteristics of very low-mass sandwich or laminated elements remains largely unaddressed. This issue becomes particularly

relevant for components such as winglets which are externally mounted structures located at the wingtip, where bending and torsional deformations reach their highest amplitudes. Owing to their position at the end of the lifting surface, winglets can noticeably affect the global dynamic response of the wing through their mass distribution, stiffness contribution, and aerodynamic interaction. Even small variations in their stiffness or attachment compliance may lead to measurable shifts in the modal properties of the entire lifting surface, especially within frequency ranges critical for aeroelastic phenomena. These considerations motivate the present work, which systematically examines the modal behavior of a composite UAV winglet under multiple support scenarios, aiming to provide practical guidance for reliably identifying physically meaningful modal parameters relevant to aeroelastic and flutter assessments.

2. Materials and Methods

The study is based on experimental vibration testing conducted to characterize the dynamic response of a composite winglet used in a mini-UAV platform. The component is manufactured as a sandwich structure with carbon fiber skins and a lightweight foam core, which results in a stiff but low-mass configuration typical for small unmanned aircraft. Due to the low mass and high compliance of such thin-walled composite assemblies, their dynamic response is highly sensitive to boundary conditions, excitation methods and measurement-induced mass loading effects.

2.1. Design of the Winglet

The winglet examined in this study is part of a Micro Class UAV (Figure 1.) designed by the team from Wrocław University of Science and Technology for the SAE Aero Design 2024 competition [19]. The aircraft follows a flying-wing configuration with a highly swept, delta-type planform, resulting in a wingspan of 0.6 m and an empty mass of approximately 1.5 kg, fully complying with the dimensional limitations defined in the SAE ruleset. A key advantage of delta wings is the sustained attachment of the flow over the wing surface at high angles of attack, which postpones stall onset and leads to improved lift characteristics and overall aerodynamic performance [20].



Figure 1. Micro Class UAV designed by Wrocław University of Science Technology student team for SAE Aero Design 2024.

In Micro category, aerodynamic efficiency is a key performance factor due to the strict take-off and payload constraints. For this reason, small tip devices were incorporated into the design to mitigate wingtip vortex formation and improve overall lift-to-drag characteristics. In addition, the winglet contributes to the control of leading-edge vortex development by limiting their outward convection towards the wingtip, thereby promoting a more effective utilization of the lifting surface.

The composite winglet analysis in the present work is one of these components and serves as an externally mounted aerodynamic extension at the wingtip.

The geometric layout as well as the physical model of the winglet is presented in Figure 2., showing all relevant dimensions. The component was designed to enhance aerodynamic performance by reducing drag and improving directional stability at the wingtips, and providing a secondary contribution to lift through the modification of local flow structures. While these design choices were made to optimize flight efficiency, the present study focuses exclusively on the dynamic characteristics of the winglet itself. Consequently, the discussion does not elaborate further on the aerodynamic rationale or detailed geometric optimization, as these aspects are outside the scope of this work. It is mounted to the wing using screws inserted through the 2 holes indicated on the Figure 2.

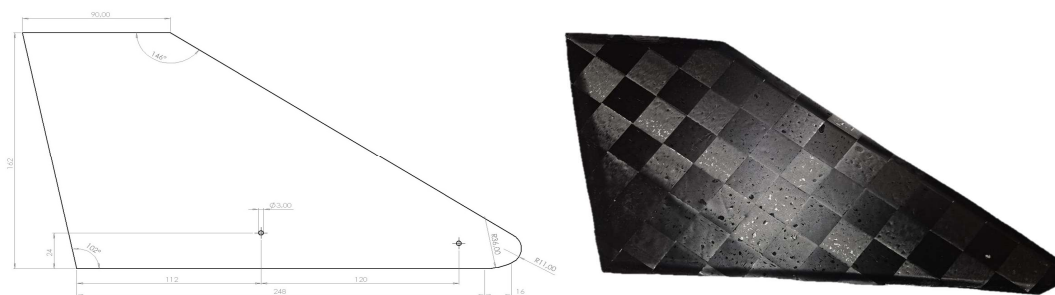


Figure 2. Geometry of the winglet.

The winglet is constructed as a sandwich structure, consisting of CFRP face sheets made from Aspro spread tow A-80 fabric arranged in a $\pm 45^\circ$ lay-up and a 2 mm Herex foam core (Figure 3). The CFRP skins provide high bending stiffness and strength, while the foam core maintains the shape and contributes to overall structural rigidity with minimal mass. The component was manufactured using a combination of hand lay-up for the CFRP layers and vacuum bagging techniques to consolidate the sandwich assembly. This manufacturing approach was selected to ensure repeatable laminate quality suitable for lightweight UAV structures. The material properties of the CFRP skins and the foam core are summarized in Table 1. and were taken from previous experimental characterization and validated reference data.

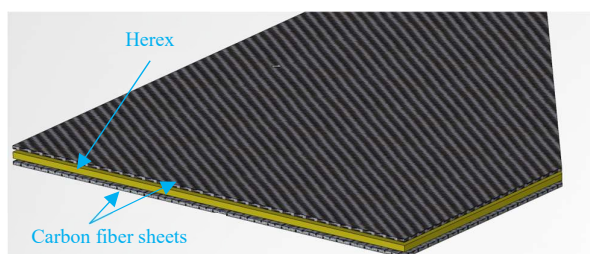


Figure 3. Sandwich structure of the winglet studied in this work.

Table 1. Material properties based on previous work [21].

Property	Aspro A-80	Herex
Density [g/cm^3]	1.79	0.06
Young Modulus E_x [MPa]	48385	70
Young Modulus E_y [MPa]	48385	70
Shear Modulus G_{xy} [MPa]	4232	58
Poisson Ratio [-]	0.04	0.3

2.2. Experimental Campaign

The experimental investigation was structured as a series of modal tests conducted under three different boundary condition configurations in order to assess their influence on the identified dynamic characteristics of a lightweight composite winglet. Due to the sandwich configuration of the structure (CFRP–Herex–CFRP), an additional measurement procedure was incorporated into the experimental campaign. In this procedure, response points were placed on both sides of the winglet (i.e., on each CFRP face sheet) to enable detailed assessment of the natural frequencies, global and local mode shapes, and the corresponding modal displacements. The measurement points shown in Figure 4 were mirrored on the opposite side of the winglet to permit direct, point-to-point comparison between the two outer skins. The actual distance between two measurement surfaces presented in Figure 5 was defined by the thickness of the test sample however, to improve the quality of presentation, the distance between the two sides of the test surfaces was scaled in the modal geometry model.

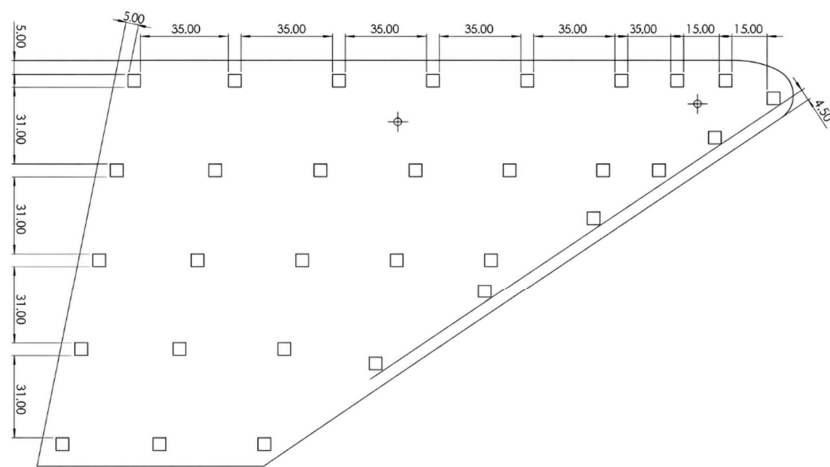


Figure 4. Measurements points.

The presented above approach applies for sandwich structures, as the two CFRP face sheets may exhibit out-of-phase motion in some mode shapes, especially at higher frequencies where the mode shape is more complex. An antisymmetric response of the two face sheets cannot be detected in case of measurements are taken only at one side of the structure. Measurements on both sides of the composite should provide more information on the vibrational behavior of the composite sandwich and allow for accurate identification of both global and local sheet modal phenomena. A comparison between the results obtained from the single-sided and double-sided analyses should highlight the potential practical implications and inform directions for future work.

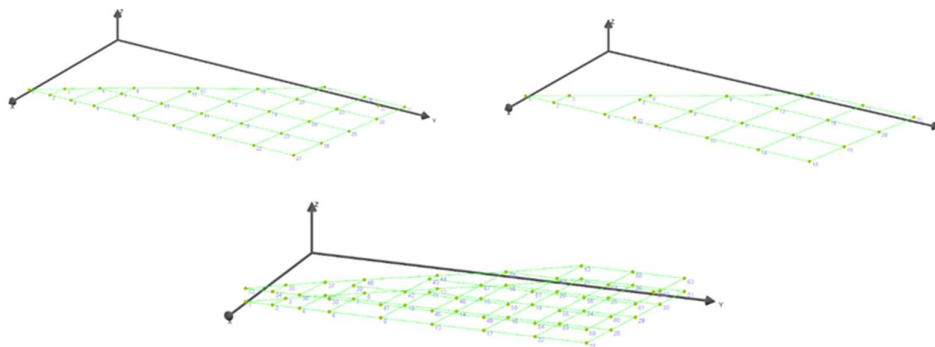


Figure 5. Measurement points located on one side and on both sides of the winglet.

Consideration of the previously discussed testing approaches should reflect the practical challenges encountered during modal testing of low-mass sandwich structures and provide a basis for formulating recommendations regarding suitable testing configurations for UAV components.

2.3. Free – Free Suspension Using Elastic Cords

In the first configuration, the winglet was tested under nominal free–free boundary conditions by suspending it using soft elastic cords (Figure 6). This setup minimizes constraint forces and stiffness contributions from the supports, allowing the intrinsic dynamic behavior of the structure to be captured. Such a configuration is commonly regarded as the reference condition for experimental modal analysis, as it enables direct comparison with numerical models formulated under unconstrained conditions.



Figure 6. Free–free suspension of the winglet using elastic cords.

2.4. Free – Free Approximation Using Flexible Foam Support

In the second configuration, the winglet was placed on a soft, highly compliant prismatic patterned foam sheet (Figure 7). Prism foam pads are commonly used in modal testing to provide minimal reaction forces, thereby approximating free–free boundary conditions while offering stable and practical testing arrangement. This setup reflects a commonly used alternative in laboratory environments.



Figure 7. Winglet supported on a soft prismatic foam, with modal hammer with interchangeable impact tips.

2.5. Fixed Boundary Conditions

In the third configuration, the winglet was tested under fixed boundary conditions by rigidly clamping it at the mounting interface (Figure 8), reproducing the operational attachment to the wing structure. This configuration represents an approximation of in-service condition of the component and allows the assessment of how boundary constraints alter the natural frequencies and mode shapes relative to the free-free cases. The comparison between fixed and free-free results provides insight into the role of mounting stiffness and load transfer on the dynamic response of wingtip devices in UAV applications.

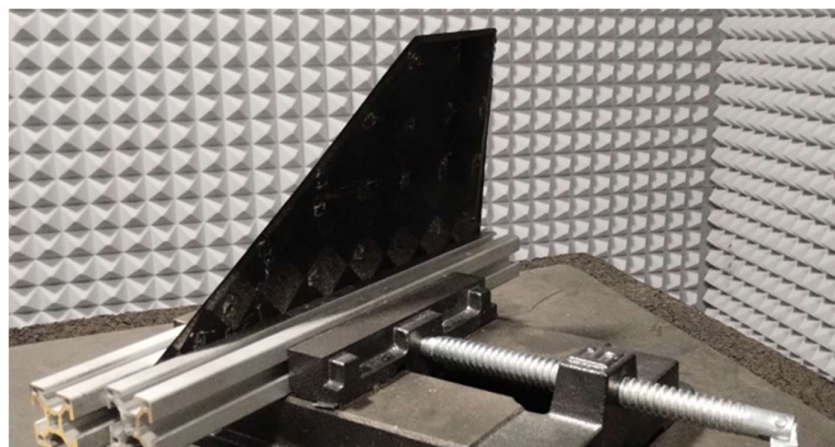


Figure 8. Winglet rigidly clamped.

For all test configurations, frequency response functions (FRFs) were computed from the measured force and acceleration signals. The resulting FRFs were subsequently used for modal parameter identification, including natural frequencies and corresponding mode shapes. The adopted measurement grid and testing procedure were designed to ensure sufficient spatial resolution and data consistency for reliable comparison between experimental configurations as well as with the numerical modal analysis.

2.5. Impact Test – Preliminary Results

The modal impact hammer presented in Figure 7 can be equipped with various interchangeable impact tips: hard stainless steel, medium-hard aluminum, medium-hard polymer, soft elastomer, and super-soft elastomer. Tip material influences the contact duration and thus the usable excitation

bandwidth. Hard tips provide short contact time and usable input spectrum also at higher frequencies, where soft rubber tips increase contact time at impact what can lead to insufficient excitation at higher-order modes.

Preliminary impact tests indicated that the hard aluminum tip provided the best quality, of excitation. To obtain broadband excitation of the CFRP plate while minimizing the risk of surface damage, the structure was excited using a modally tuned impact hammer equipped with an aluminum tip which delivers the broad range input without high impact forces as in case of stainless-steel tips, which increase local contact stresses and thus the risk of surface damage or delamination [22,23].

The lightweight nature of the CFRP wing structure initially suggested the use of a low-mass miniature impact hammer. However, preliminary impact testing showed that the structure failed to provide a reliable accelerometer response due to insufficient energy transfer. To address this issue, an additional 25 g extender mass was added to the modal hammer to increase the impact amplitude and achieve broad, stable excitation across the frequency range of interest. In all configurations, the winglet was excited using a modal impact hammer (PCB 086C01), using roving accelerometer method, where the excitation point was constant during each test set.

For each measurement point, three consecutive hammer impacts were applied, and the corresponding frequency response functions were averaged to improve the repeatability of the identified modal parameters. The structural response was measured using a miniature triaxial piezoelectric accelerometer (PCB 356A03) [24], sequentially repositioned to predefined measurement locations distributed over the winglet surface (Figure 4). Frequency response functions (FRFs) were computed from the acquired force and acceleration signals and subsequently used for modal parameter identification, including natural frequencies and corresponding mode shapes.

The use of a 1 gm triaxial miniature accelerometer on lightweight structures introduces added mass and can measurably influence the systems response. A non-contact response measurement method, such as Laser Doppler Vibrometry (LDV), avoids accelerometer-induced mass loading, unfortunately its application to structures tested under free-free boundary conditions present several methodological challenges. In some cases, the test object is supported on elastic bands (e.g., soft foam or elastic cords) to approximate a free-free support condition. Relative motion of the test object in regard to the LDV unit can disrupt vibrometer signal stability, especially in case CFRP low-reflective and curved surfaces. Although vibrometry is advantageous for eliminating mass-loading effects, careful environmental isolation, optical target preparation, and stabilization of the free-free support system are essential to ensure measurement integrity.

For this preliminary research stage, the 1 gm triaxial accelerometer was selected to measure the structural responses. This choice provides stable and repeatable measurements without the optical alignment challenges and relative displacement of the sample - LDV unit. It is worth noting that the authors explicitly acknowledge and account for the potential influence of the accelerometer on the measured dynamic response. The use of a triaxial sensor allowed the simultaneous acquisition of acceleration components in three orthogonal directions, enabling the identification of both bending- and torsion-dominated vibration modes. Particular attention was paid to maintaining consistent sensor orientation and attachment conditions during the measurements, as the low mass of the structure makes the results sensitive to local mass perturbations. During the initial phase of each test configuration – each support condition of the winglet – the modal hammer force-time signal and power spectrum density were analyzed to verify the quality of the system excitation. Figure 9 presents the excitation forces recorded at the impact-hammer force sensor during excitation achieved at each support condition.

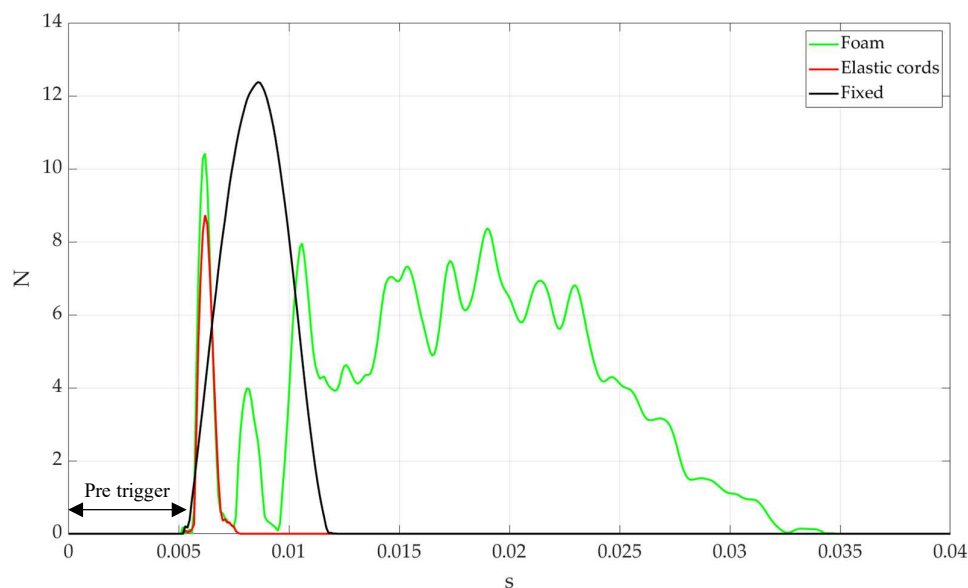


Figure 9. Measured impact-hammer force signals for the different winglet support conditions.

In the case of the soft foam support, it was impossible to achieve good-quality excitation, as numerous impacts are visible. The prismatic patterned foam used for support created a strong damping support condition that prevented efficient force transmission from the impact hammer. The prism patterning of the foam introduces numerous small contact points with the test object, which increase energy dissipation during impact. As a result, when the hammer strikes the structure, a significant portion of the input energy was absorbed or redirected by the deformable foam instead of being transmitted into the structure. This led to multiple hammer impacts, extended contact durations, and a significant reduction in mid- and high-frequency content. In the case of the fixed support, it was possible to introduce a single-impact excitation, although much effort was needed to prevent double impacts in free-hand operation. The excitation impulse is also wider than in the case of the free-free condition achieved by means of elastic cords.

Reciprocity analysis was used to verify the linearity and stability of the test setup at the free-free support condition. FRFs obtained for point A (driving point) to point B (response) were compared to the FRFs obtained in the reverse direction point B (driving point) to point A (response). Three pairs of points (18–25, 20–8, 28–20) were analyzed for the free-free elastic bands support condition. In all analyzed cases (Figure 10–Figure 12), the reciprocity test reveals differences in FRF amplitude and frequency. It can be stated that the main reason for the identified non-reciprocity is the mass loading caused by the roving accelerometer. Although the main acceleration peaks are still visible in the spectrum, frequency shifts are visible. The modal mass at resonances, which is the effective mass associated with a vibration mode at the measurement point, is comparable with the accelerometer mass, causing visible mass loading. Another point to consider in the case of non-reciprocity are double hammer impacts, unstable boundary conditions, structural nonlinearities, and delamination. First two causes can be deemed irrelevant—double-hit warning conditions were set at the measuring system and each hammer hit was thoroughly investigated for double impact. The support condition was not modified throughout the test procedure. Structural nonlinearities due to matrix micro-cracking or delaminations cannot be ruled out nor confirmed, as mass loading due to the roving accelerometer is surely present in the system.

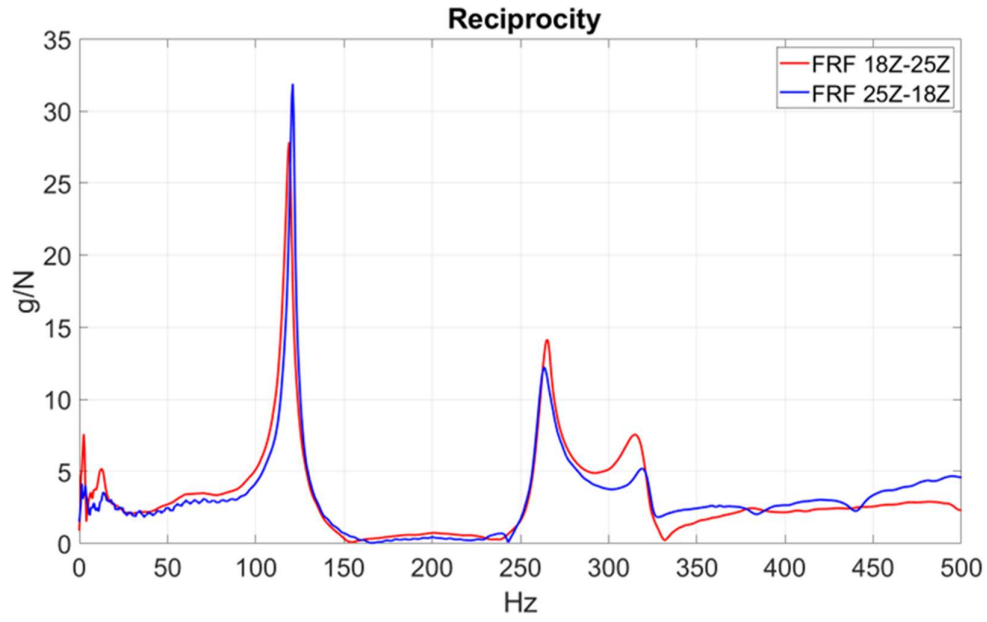


Figure 10. FRF reciprocity comparison – Points 18 and 25, Z axis.

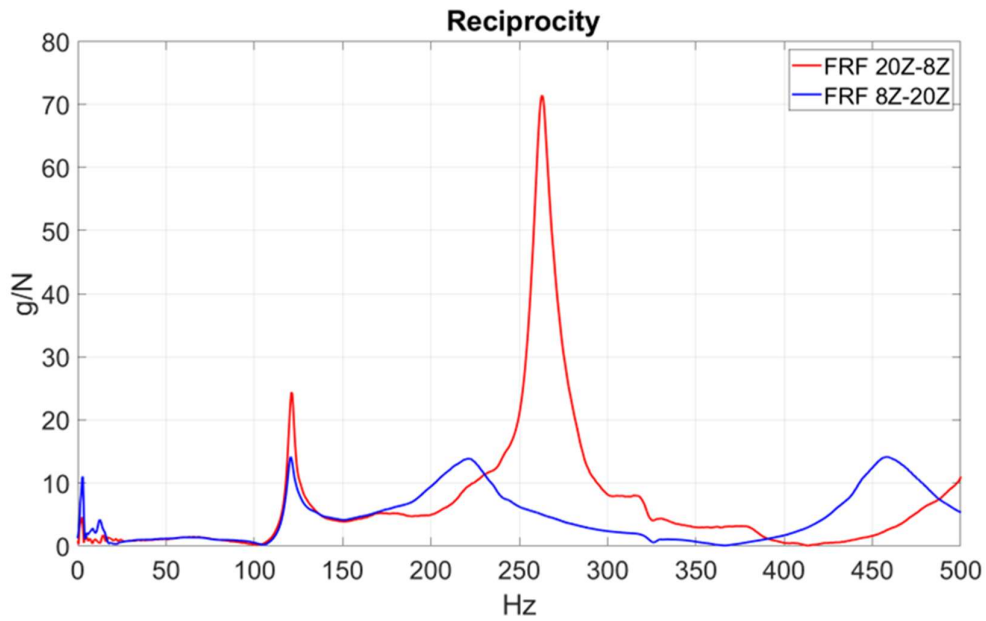


Figure 11. FRF reciprocity comparison – Points 8 and 20, Z axis.

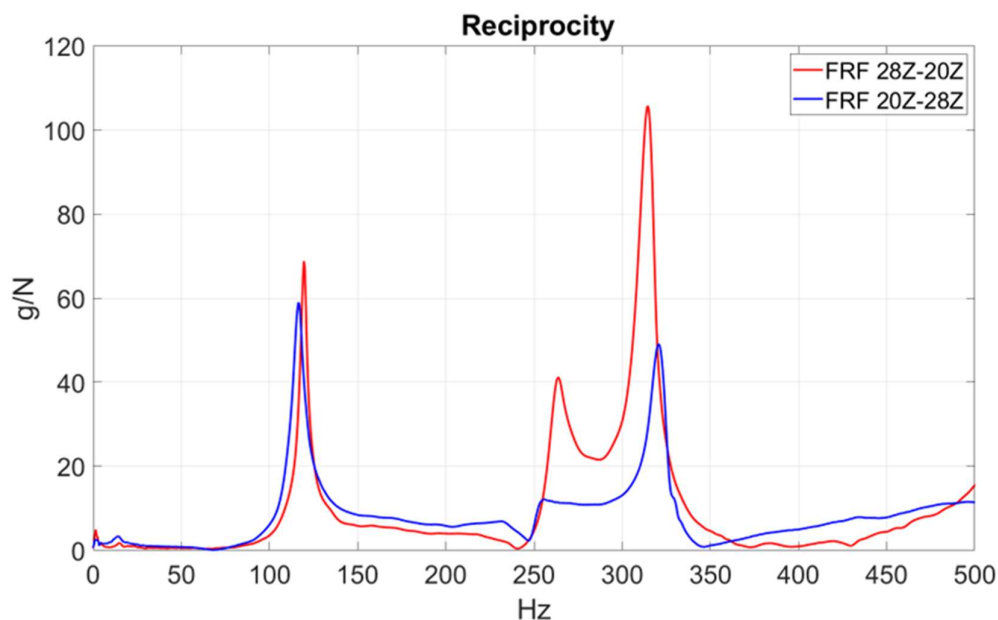


Figure 12. FRF reciprocity comparison – Points 28 and 20, Z axis.

Although the visible non-reciprocity and test setup limitations, the experimental testing was conducted due to the preliminary character of the research, where the main objective is to assess the usefulness of the test setup, excitation method, and data acquisition. Further structural testing was conducted to explore limitations and challenges in structural testing of lightweight composite structures. At this point, it is already clear that future work should incorporate reduced mass loading, refined support conditions, and further analysis of structural nonlinearities due to the anisotropic nature of CFRP.

3. Results

Singular Value Decomposition of the FRF matrix was implemented to compute the Complex Mode Indicator Function (CMIF) for each test setup. At each instance the number of FRFs is different due to the number of response points. Dominant singular values at modal frequencies become numerically larger as the number of response points, and thus the number of FRFs, increases. In order to compare the CMIF functions calculated for each test condition, a max-min normalization was conducted to improve the visual representation of the data.

As visible in Figure 13, in the case of the free-free condition the CMIF function peaks around 260 Hz for both free test conditions. The introduction of additional response points at the CFRP—measurements conducted on both sides of the winglet—did influence the shape of the CMIF function. At the dominant peak, it splits into two sub-peaks in the case of the double-sided test setup. Further investigation of the mode shapes occurring at the two sub-peaks reveals a similar mode shape (Figure 14), and the Modal Assurance Criterion of those two modes equals 0.57, which indicates one mode but obtained under altered measurement conditions such as mass loading and changes in local bending curvature.

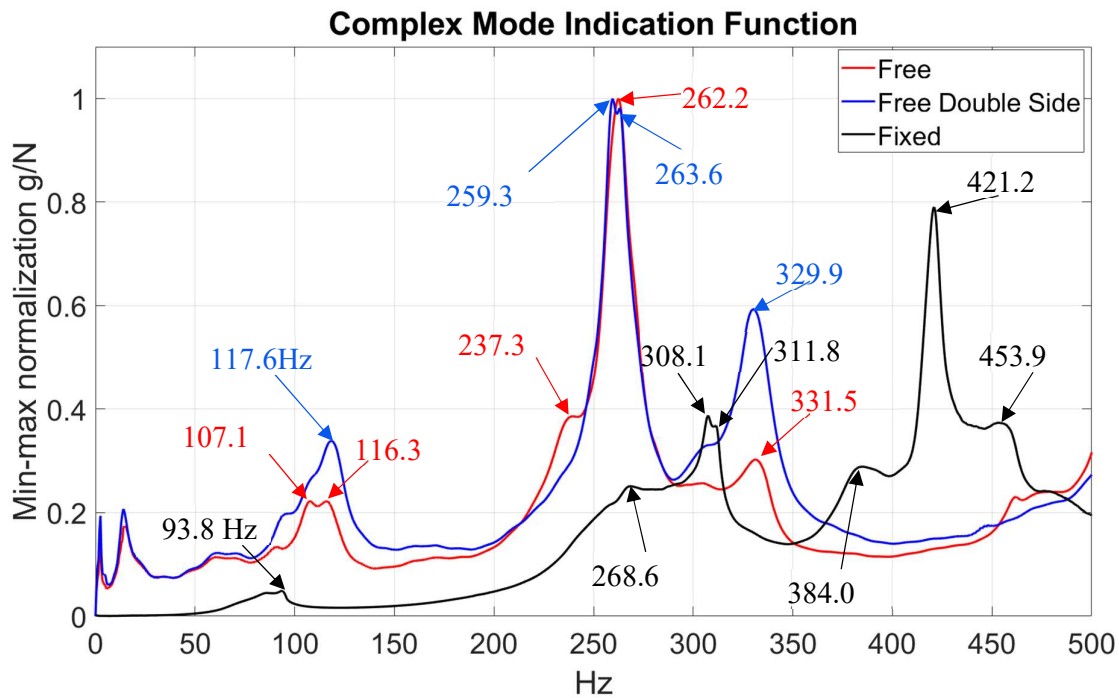


Figure 13. Complex Mode Indicator Function at various support conditions.

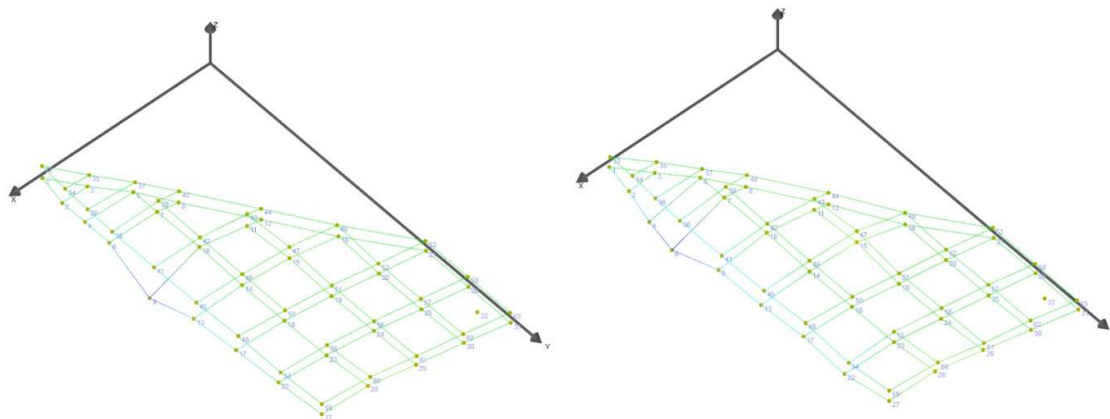


Figure 14. Mode shapes at two sub peaks 259.3 Hz and 263.6 Hz

Main displacement alongside the longer side of the winglet. No visible vibration in other points of the object. The first two modes visible below 50 Hz in case of both free conditions represent rigid-body motion caused by the stiffness of the elastic cords and their length. In the case of the single-sided free support condition, two modes are present at 107.1 Hz and 116.3 Hz consequently. At first glance both identified mode shapes are similar (Figure 15), but detailed analysis of the mode-shape animation shows a more complex shape occurring at 116.3 Hz, where displacement is visible not only at the tip of the winglet but also at the opposite edge. The MAC value for those two modes is equal to 0.19, also indicating two separate modes.

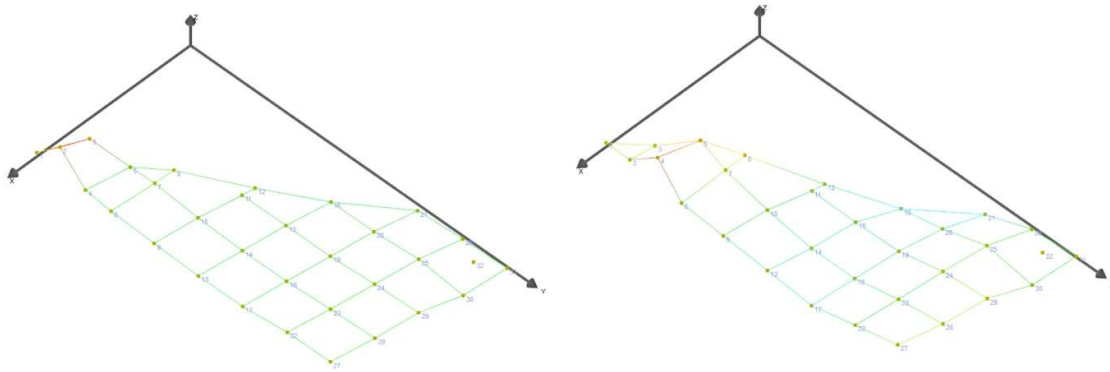


Figure 15. Mode shapes at 107.1 Hz and 116.3 Hz.

Additional FRFs included in the CMIF computation for the double-sided response caused changes in this frequency range what caused a more pronounced peak is visible at 117.6 Hz, making it the dominant frequency in this region. The mode occurring at 116.3 Hz for the single-sided measurement was shifted upward to 117.6 Hz, as a detailed analysis of the mode-shape animations indicates the same shape (Figure 16). The CMIF value at 117.6 Hz is also higher due to the increased number of FRFs used in the computation.

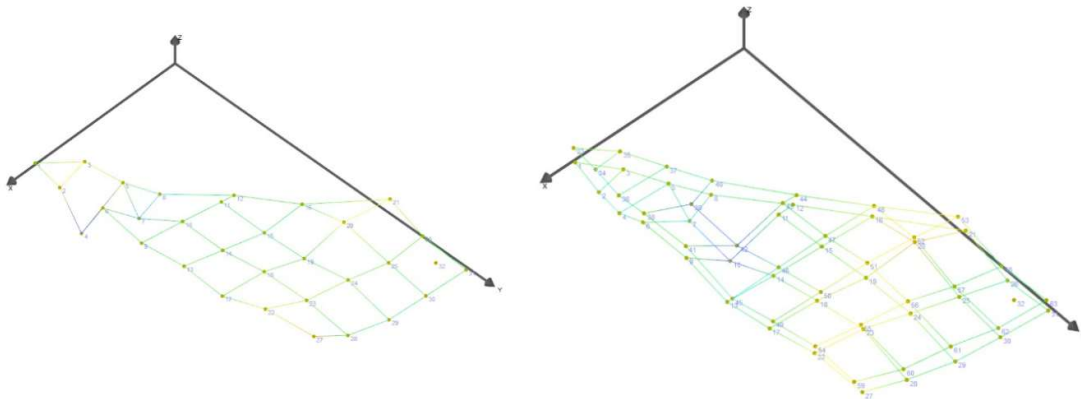


Figure 16. Mode shapes at 116.3 Hz – single side response and 117.6 Hz – double side response.

Further comparison of the CMIF peaks indicates modes at 331.5 Hz for the single-sided measurement and 329.9 Hz for the double-sided response (Figure 17). In this case, a frequency shift is also visible, as the mode-shape animation presents similar patterns. Once again, the CMIF values are greater for the double-sided responses, which is to be expected.

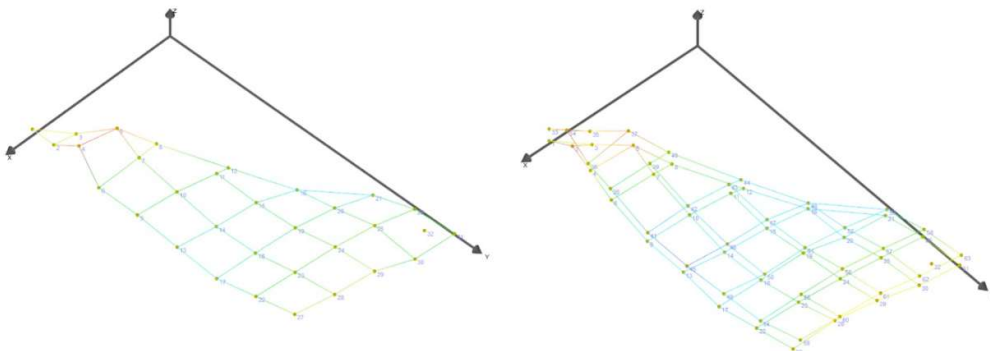


Figure 17. Mode shapes at 331.5 Hz – single side response and 329.9 Hz – double side response.

A significant difference in the CMIF is visible in the case of the fixed-support condition. As presented in Figure 8, the longer edge of the winglet was clamped in a vise, significantly reducing the area of the winglet that can respond to impacts. The first modes identified in the free condition were concentrated around the winglet tip. Since the tip of the winglet is fixed in the vise, the first mode differs substantially in both frequency and shape. Figure 18 presents the first mode shape identified for the fixed condition at 93.8 Hz, which consists of bending of the winglet around the Y-axis.

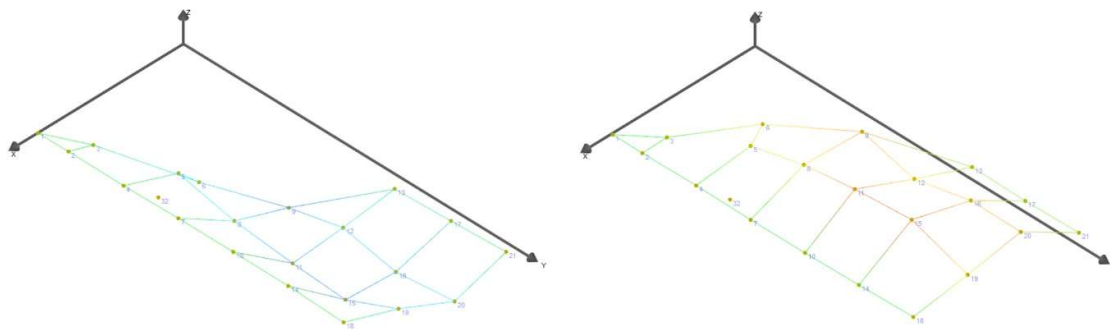


Figure 18. Mode shapes at 93.8 Hz – single mode at two to end positions.

The dominant peak of the fixed-support CMIF function is shifted to higher frequencies compared with both free-support conditions. The main peak was identified at 421,2 Hz, and the corresponding mode shape is shown in Figure 19. This mode shape can be compared in form and complexity to the modes at 331.5 Hz for the single-sided response and 329.9 Hz for the double-sided response, presented in Figure 17. Naturally, due to the clamping of the winglet, the portion of the structure able to respond to excitation is smaller than in the free-free condition. The resulting change in effective geometry, and the associated increase in stiffness, shifts the mode frequency to higher values.

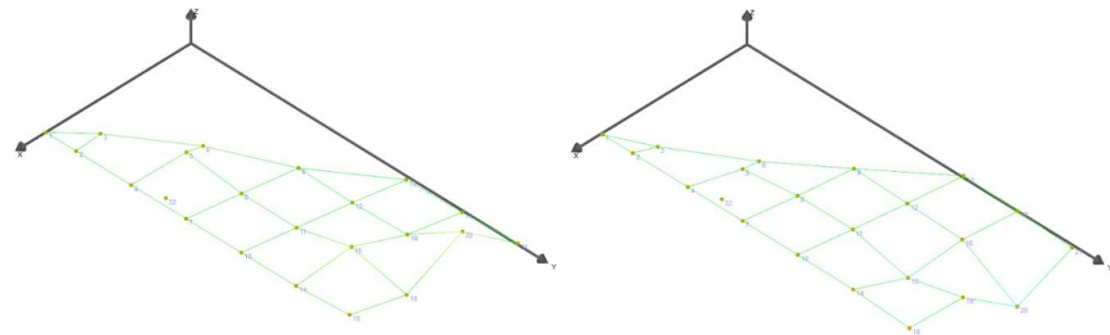


Figure 19. Mode shapes 421.2 Hz – single mode at two to end positions.

4. Conclusions

The experimental results demonstrate that boundary conditions constitute a key factor that influences the dynamic characteristics of the composite winglet. The transition from free-free conditions to a rigidly fixed configuration resulted in a significant shift of the dominant modal frequencies toward higher values (from 260 Hz to 420 Hz). In the fixed configuration, the longest edge of the winglet was rigidly clamped, which substantially increased the overall stiffness of the structure and altered the effective mass participation in vibration (Figure 19). Modes that were

dominated by the winglet tip under free–free conditions were strongly affected, as the tip region became clamped in the fixed configuration.

The free–free approximation based on prismatic foam support proved to be unsuitable for the investigated lightweight sandwich structure. The foam introduced excessive damping and dissipated a substantial portion of the input energy during impact excitation, which led to multiple hammer contacts and prolonged force duration (Figure 9). As a result, modal identification under this configuration was unreliable. This finding indicates that such a support method is inappropriate for lightweight composite structures.

Double-sided response measurements revealed measurable differences in the identified modal characteristics at higher frequencies compared to single-sided measurements. The observed peak splitting and frequency shifts in the CMIF are attributed to a combination of factors: phase-shifted or locally antisymmetric motion of the CFRP face sheets characteristic of sandwich structures, measurement-induced mass loading effects, and unavoidable geometric imperfections in mirroring measurement points on opposite sides of a thin structure. The results indicate that, while double-sided measurements provide access to richer modal information, they also introduce additional sensitivity to measurement alignment and mass perturbations, which must be explicitly considered during interpretation. On the other hand, single-sided measurements provide valid information on the system dynamics, especially in the lower frequency range up to 500 Hz, where the modes exhibit global-like shapes. In the case of sandwich-type lightweight composites, single-sided measurements are generally sufficient for standard modal testing or for preliminary, fast system-dynamics identification, as fewer measurement points—and thus fewer FRFs—are required.

Double-sided response acquisition, although more demanding and time-consuming, can be beneficial for more detailed investigations, such as the analysis of local and internal damage, stiffness loss, core–skin debonding, validation of structural symmetry, and identification of mass-loading effects.

The present study demonstrates that the influence of accelerometer mass is non-negligible. For such lightweight structures, even miniature sensors alter the dynamic response in a measurable manner, particularly in higher-frequency regimes. This confirms that conventional assumptions regarding negligible sensor influence are not valid for ultra-light composite UAV components.

The quality of modal excitation was found to be a critical factor for reliable identification of the dynamic characteristics of the lightweight composite winglet. The selection of the impact hammer tip material had a direct influence on the achievable excitation bandwidth, as softer tips led to prolonged contact durations and insufficient high-frequency content, while overly hard tips increased the risk of local surface damage. Among the tested configurations, the aluminum impact tip provided the most favorable compromise between broadband excitation and structural safety, enabling effective excitation of both low- and higher-order modes.

Furthermore, the study demonstrated that the low mass of the structure imposes limitations on the use of miniature, low-energy impact hammers. Preliminary tests showed that insufficient energy transfer resulted in poor accelerometer response and reduced repeatability of the measured FRFs. The introduction of an additional extender mass on the modal hammer significantly improved excitation stability and force amplitude, allowing for consistent broadband input across the frequency range of interest. These findings indicate that, for ultra-light composite structures, excitation force levels must be carefully adjusted to ensure adequate energy input while avoiding excessive local stresses, and that hammer mass and tip selection constitute essential parameters of the experimental setup.

The sandwich construction itself plays an important role in shaping the observed dynamic response. The foam core not only contributes to bending stiffness but also introduces distributed material damping, which affects excitation efficiency, modal bandwidth, and the clarity of resonance peaks. Future research should focus on the use of non-contact response measurement techniques, such as Laser Doppler Vibrometry, to eliminate sensor-induced mass loading and enable more accurate modal identification. A direct, quantitative comparison between LDV-based and

accelerometer-based measurements under identical boundary conditions is required to isolate measurement-related effects from the true structural behavior.

Further work should also extend modal testing to operational configurations in which the winglet is mounted on the complete wing or aircraft structure. Such tests would allow a more realistic capture of the interaction between the winglet and the supporting structure and would provide modal data directly relevant to aeroelastic and operational analyses.

From a numerical perspective, high-fidelity finite element models should be developed and correlated with the experimental results, incorporating layered composite behavior, foam core damping, and realistic boundary stiffness.

Taken together, these directions would enable a more comprehensive understanding of the dynamic behavior of lightweight sandwich wingtip devices and support the development of reliable experimental and numerical methodologies tailored to next-generation unmanned aerial vehicle structures.

Author Contributions: Conceptualization, J.W., A.K., M.S. and O.P.; methodology, J.W., K.J., M.K. and M.M.; software, J.W., K.J. M.M. and O.P.; validation, J.W., A.K., M.S, O.P., and M.K.; formal analysis, M.S. and M.K.; investigation, J.W., K.J., and M.M.; resources, O.P. and A.K.; data curation, J.W., K.J., M.S and O.P.; writing—original draft preparation, J.W., K.J., M.M.; writing—review and editing, A.K., M.S., O.P. and M.K.; visualization, J.W and M.M; supervision, A.K., M.S., O.P. and M.K.; project administration, A.K. and O.P. All authors have read and agreed to the published version of the manuscript.

Funding: This research received no external funding.

Data Availability Statement: The data will be available on request.

Conflicts of Interest: The authors declare no conflicts of interest.

References

1. Guerrero-Sánchez, M.-E.; Hernández-González, O. Dynamics and Control of UAVs. *Machines* **2024**, *12*, 749, doi:10.3390/machines12110749.
2. Saponi, M.; Borboni, A.; Adamini, R.; Faglia, R.; Amici, C. Embedded Payload Solutions in UAVs for Medium and Small Package Delivery. *Machines* **2022**, *10*, doi:10.3390/machines10090737.
3. Deng, H.; Huang, J.; Liu, Q.; Zhao, T.; Zhou, C.; Gao, J. A Distributed Collaborative Allocation Method of Reconnaissance and Strike Tasks for Heterogeneous UAVs. *Drones* **2023**, *7*, doi:10.3390/drones7020138.
4. Gargalakos, M. The Role of Unmanned Aerial Vehicles in Military Communications: Application Scenarios, Current Trends, and Beyond. *Journal of Defense Modeling & Simulation* **2024**, *21*, 313–321, doi:10.1177/15485129211031668.
5. Colomina, I.; Molina, P. Unmanned Aerial Systems for Photogrammetry and Remote Sensing: A Review. *ISPRS Journal of Photogrammetry and Remote Sensing* **2014**, *92*, 79–97, doi:10.1016/j.isprsjprs.2014.02.013.
6. Kovalev, I.V.; Voroshilova, A.A.; Karaseva, M.V. Analysis of the Current Situation and Development Trend of the International Cargo UAVs Market. *J. Phys.: Conf. Ser.* **2019**, *1399*, 055095, doi:10.1088/1742-6596/1399/5/055095.
7. Elham, A.; van Tooren, M.J.L. Winglet Multi-Objective Shape Optimization. *Aerospace Science and Technology* **2014**, *37*, 93–109, doi:10.1016/j.ast.2014.05.011.
8. Kumpati, R.; Skarka, W.; Skarka, M.; Brojan, M. Enhanced Optimization of Composite Laminates: Multi-Objective Genetic Algorithms with Improved Ply-Stacking Sequences. *Materials* **2024**, *17*, doi:10.3390/ma17040887.
9. Nikolaou, E.; Karatzas, E.; Kilimtzidis, S.; Kostopoulos, V. Winglet Design for Class I Mini UAV—Aerodynamic and Performance Optimization. *Engineering Proceedings* **2025**, *90*, doi:10.3390/engproc2025090111.
10. González, P.; Chaves Barbosa, G.; García Quesada, Á.; Stavorinus, G.; Silvestre, F.; Hilger, J.; Hanke, C.; Voß, A.; Krüger, W. Wind Tunnel Testing and Modal Validation of TU-FLEX'S High Aspect-Ratio Wings.

- In Proceedings of the International Forum on Aeroelasticity and Structural Dynamics IFASD 2024; 17-21 June 2024, The Hague, The Netherlands.
11. Maharudra; Arya, B.; Rajanna, T. Effect of Ply-Orientation and Boundary Conditions on the Vibrational Characteristics of Laminated Composite Panels Using HODST. *Materials Today: Proceedings* **2020**, *20*, 134–139, doi:10.1016/j.matpr.2019.10.062.
 12. Guo, Z.; Sheng, M.; Zhang, K. Effect of Boundary Conditions on Vibration Characteristics of a Sandwich Plate with Viscoelastic Periodic Cores. *Machines* **2025**, *13*, 863, doi:10.3390/machines13090863.
 13. Erkliğ, A.; Bulut, M.; Yeter, E. The Effect of Hybridization and Boundary Conditions on Damping and Free Vibration of Composite Plates. *Science and Engineering of Composite Materials* **2015**, *22*, 565–571, doi:10.1515/secm-2014-0070.
 14. Qu, C.; Yan, Q.; Zou, X.; Gou, D.; Liu, X. Experimental Study on Modal Testing Methods for Typical Composite Honeycomb Sandwich Structures. *IJFET* **2024**, *6*, doi:10.25236/IJFET.2024.060503.
 15. Karpenko, M.; Stosiak, M.; Deptuła, A.; Urbanowicz, K.; Nugaras, J.; Królczyk, G.; Żak, K. Performance Evaluation of Extruded Polystyrene Foam for Aerospace Engineering Applications Using Frequency Analyses. *Int J Adv Manuf Technol* **2023**, *126*, 5515–5526, doi:10.1007/s00170-023-11503-0.
 16. Zhang, L.; Liao, W.; Liu, B.; Feng, S.; Fan, J. Thermal Model Test and Multi-Scale Simulation Method for the Lattice-Structured Air Rudder of Hypersonic Flight Vehicle. *Aerospace Science and Technology* **2026**. doi:10.1016/j.ast.2026.111885.
 17. Qaumi, T.; Hashemi, S.M. Experimental and Numerical Modal Analysis of a Composite Rocket Structure. *Aerospace* **2023**, *10*, 867, doi:10.3390/aerospace10100867.
 18. Chung, S.; Kim, C.-J. Evaluation of the Modal Parameters of a Unidirectional Carbon-Based Composite Structure Using the Influential Factor of Static Loading. *Materials* **2024**, *17*, 3209, doi:10.3390/ma17133209.
 19. 2024 Collegiate Design Series SAE Aero Design Rules. <https://www.sae-aerodesign.com/cdsweb/gen/DownloadDocument.aspx?DocumentID=f9dcb79b-b8d4-42b2-a1d3-2af1fb16aee7> (accessed on 2 February 2026).
 20. Gupta, S.; Kumar, S.; Kumar, R. Control of Leading-Edge Vortices over Delta Wing Using Flow Control Methods: A Review. *Materials Today: Proceedings* **2022**, *50*, 2189–2193, doi:10.1016/j.matpr.2021.09.447.
 21. Milewski, M.; Kierzkowski, A.; Kucharski, M.; Zielonka, P. Inverse Method for Material Characterization of a UAV Composite Wing Based on FEM and Dynamic Response. *Eksploracja i Niezawodność – Maintenance and Reliability* **2025**, doi:10.17531/ein/207312.
 22. Huo, L.; Alderliesten, R.; Sadighi, M. Delamination Initiation in Fully Clamped Rectangular CFRP Laminates Subjected to Out-of-Plane Quasi-Static Indentation Loading. *Composite Structures* **2023**, *303*, 116316, doi:10.1016/j.compstruct.2022.116316.
 23. Brooks, R.A.; Liu, J.; Hall, Z.E.C.; Joesbury, A.M.; Harper, L.T.; Liu, H.; Kinloch, A.J.; Dear, J.P. The Relationship Between the Extent of Indentation and Impact Damage in Carbon-Fibre Reinforced-Plastic Composites after a Low-Velocity Impact. *Appl Compos Mater* **2024**, *31*, 1869–1888, doi:10.1007/s10443-024-10223-2.
 24. Miniature Triaxial ICP Accelerometer Data Sheet. Available online: https://www.pcb.com/contentstore/mktgcontent/linkedddocuments/vibration/TM-VIB-356A01-356A03_lowres.pdf?_gl=1*y16wq9*_up*MQ..*_ga*MTgyODY5NzExNC4xNzcwODMxOTIw*_ga_EZDE1W5SJT*czE3NzA4MzE5MjAkzbEkZEkdDE3NzA4MzE5MjEkajU5JGwwJGgw (accessed on 4 February 2026).

Disclaimer/Publisher's Note: The statements, opinions and data contained in all publications are solely those of the individual author(s) and contributor(s) and not of MDPI and/or the editor(s). MDPI and/or the editor(s) disclaim responsibility for any injury to people or property resulting from any ideas, methods, instructions or products referred to in the content.